ELSEVIER

Journal of Power Sources 95 (2001) 153–161

JOURNAL OF POWER SOURCES

www.elsevier.com/locate/jpowsour

High rate recharge of stationary VRLA batteries

P. Häring*, H. Giess

Oerlikon Stationary Batteries Ltd., Dornacherstr. 110, CH4147 Aesch/BL, Switzerland

Abstract

The high rate charge behavior of 6 V 155 A h lead acid monoblocs of the VRLA type for stationary service, subsequent to a full discharge in 1 h to 1.60 Vpc, is described. Charging rates with an initial constant current equal to I_{10}, $3I_{10}$, $7I_{10}$ and with constant voltage of 2.25 Vpc, resulting in a peak current of $22I_{10}$, were evaluated for their influence on the sites and magnitude of internal heating, speed of recharge and gas emission phenomena. The results indicate that recharge with an initial current in the $3I_{10}$ to $7I_{10}$ range and the maximum voltage limited to 2.25 Vpc appears to be a viable charging strategy. Full recharge can be achieved in 4–6 h with the temperature rise limited to 12°C above ambient and the gas evolution to an equivalent of 0.4 l per cell of a hydrogen–33% oxygen mixture. The thermal video imaging revealed that the loci of maximum internal heating reflect the IR drop and the heat loss through top lead and monobloc walls.

Keywords: Lead acid battery; VRLA; Thermal video imaging; Constant current; Constant voltage; Recharge speed; Gas emission

1. Introduction

Stationary lead acid batteries of the VRLA–AGM type have a low internal resistance (0.3–0.8 mΩ per 100 A h C_{10} and cell) and associated very good high rate performance (35–45% of the 10 h capacity dischargeable in 10 min) when compared to the traditional European flooded stationary battery design. This type of performance makes such batteries attractive for uninterruptible power system (UPS) service. In such an application the battery supplies power during mains outages lasting from microseconds to 1 h. As per definition these power outages are unpredictable in terms of their length and occurrence and synonyms of potential mains power instabilities, one key operational requirement for such batteries is that they should be rechargeable in a very short time. Fast recharge to a high state of charge allows to quickly brace for yet another mains disturbance and thus protect the electrical and electronic equipment from power loss also on the long run.

High rate recharges can be associated however with significant internal heating and excessive gas evolution which, in the case of VRLA batteries, enhances dry-out of the electrolyte.

The present study quantifies these phenomena so to optimize the charging strategy for the achievement of a high state of charge and a long service life and extends the knowledge of the possible beneficial effects of high rate charging reported in previous studies [1–3].

The measurements were carried out on a stationary VRLA monobloc with 6 V and 155 Ah C_{10} (1.80 Vpc at 20°C) capacity. The monobloc was discharged at room temperature with the 1 h rate of 116 A to 1.60 Vpc and recharged with an initial constant charging current ranging from I_{10} to $7I_{10}$ and with the voltage limited to 2.25 Vpc. One recharge experiment was carried out with constant voltage charging and an associated peak current of $22I_{10}$.

2. Experimental

The battery used in these experiments was a commercial 6 V VRLA monobloc manufactured by Oerlikon Stationary Batteries Ltd. Switzerland with 155 Ah C_{10} (1.80 Vpc at 20°C) capacity in flat plate construction with the electrolyte immobilized in a glass mat (AGM) and assembled in an ABS monobloc case. The discharge/charge sequences were carried out at room temperature of approximately 23–25°C after several days of float charge operation at 2.25 Vpc.

The discharge at 116 A to 1.60 Vpc allowed to withdraw 75% of the rated 10 h capacity in 1 h and represented the upper limit of duration of an UPS type discharge service. The recharge was carried out, immediately after

* Corresponding author. Tel.: +41-61-706-36-36; fax: +41-61-706-36-92.
E-mail addresses: p.haering@accuoerlikon.com (P. Häring), h.giess@accuoerlikon.com (H. Giess).

0378-7753/01/$ – see front matter
PII: S0378-7753(00)00615-7

the termination of discharge, under IU conditions of constant current of 15.5 A (I_{10}), 46.5 A ($3I_{10}$), 108.5 A ($7I_{10}$), to the maximum voltage of 2.25 Vpc and under U = constant condition with a constant voltage and a peak charging current of 341 A.

The monobloc was enclosed in a cubicle made of polystyrene foam except for one face which was exposed to the free flow of ambient air at 0.2 ms^{-1} and which was looked at with the thermal imaging video system. The connections to the monobloc terminals were made with copper connectors of 180 mm^2 cross-section so to prevent undue heat generation in these external conductors.

The discharge equipment used was a fully programmable electronic load of the type HEW 60/700 made by Digatron (Germany) and charging was carried out with an constant current–constant voltage power source of the type TCR 10T750 made by Electronic Measurements (USA) with 750 A maximum current at 10 V.

The temperature of each of the three cells was monitored with J-type thermocouples made by Philips (The Netherlands) and mounted correspondingly on the side wall of the monobloc case.

The gas emitted from the cell via the valves was collected and carried through a piping to a common water volume displacement vessel (inverted burette type). The equivalent amount of displaced water from this vessel flowed, with a fixed hydrostatic head of 20 mm, into a container on an electronic balance with 0.1 g resolution of the type PM3000/9325 by Mettler Toledo (Switzerland). The balance was equipped with an analog signal output channel and the volume of gas emitted was recorded as function of time as the weight of water collected in the container on the balance.

The pressure inside two of the three cells of the monobloc (cell 1 and cell 3) was measured with an electronic pressure gauge of the type ED505/314.412 with 0–1 bar/0–10 V range made by Haenni (Switzerland) and directly mounted on the monobloc.

The oxygen content of the emitted gas was determined with a flow-through, non-destructive, paramagnetic oxygen gas analyzer of the type Helox 2-S made by MBE Electronics (Switzerland). For this purpose the gas emitted from the cells was first carried through the oxygen analyzer and then quantitatively collected in the gas displacement vessel.

All the data signals of the analyzed parameters were collected in parallel in a strip chart mode with a PC controlled data acquisition unit of the type HP34970A and the software tool Bench Link made by Hewlett Packard (USA). This recording mode allowed to easy correlate the timing of each change in parameter values.

The thermal video imaging system used was of the type TVS-2000 MK2 made by Avio (Japan) and already described extensively in [4]. The thermal imaging exploited the fact that ABS is essentially transparent to the analyzed infrared radiation and thus allows to look at the interior cell components, directly and hence to determine their temperature and its distribution.

The experimental set-up is shown in Figs. 1 and 2 shows the monobloc as viewed at by the thermal video imaging camera. The plate stack within each cell is oriented perpendicularly to the exposed monobloc side.

3. Results

3.1. Thermal effects

3.1.1. Temperature evolution

Lead acid batteries generate heat during charge and discharge due to electrochemical polarization effects and Ohmic losses. Lead acid batteries of the VRLA type create additional heat due to the oxygen recombination cycle to the tune of approximately 0.1 W per cell and 100 Ah C_{10} capacity.

Temperature rises in such batteries have to be properly managed so to prevent an escalating current and temperature

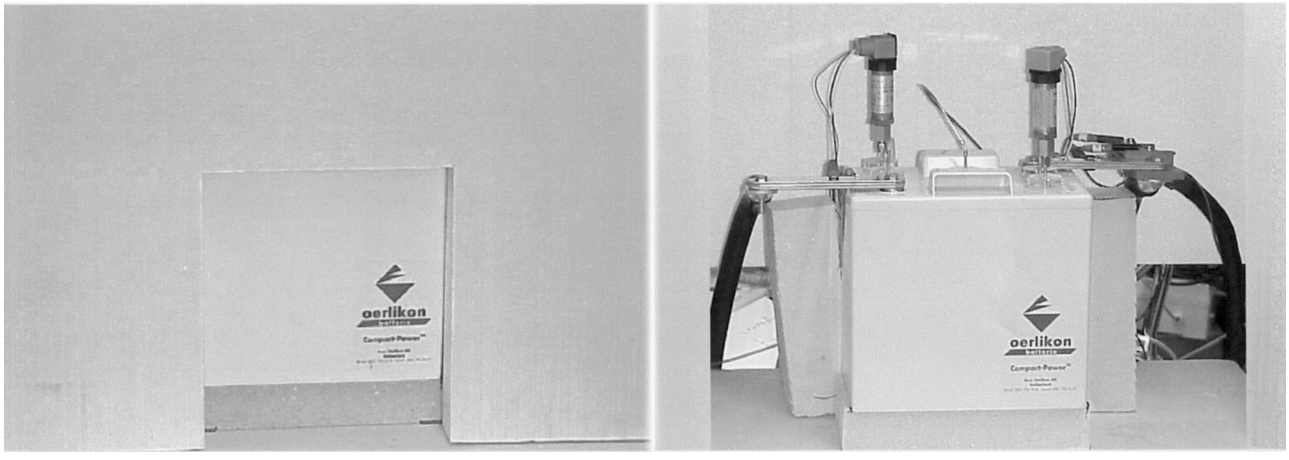

Fig. 1. Set-up of the monobloc surrounded by the PS foam cubicle and an exposed surface.

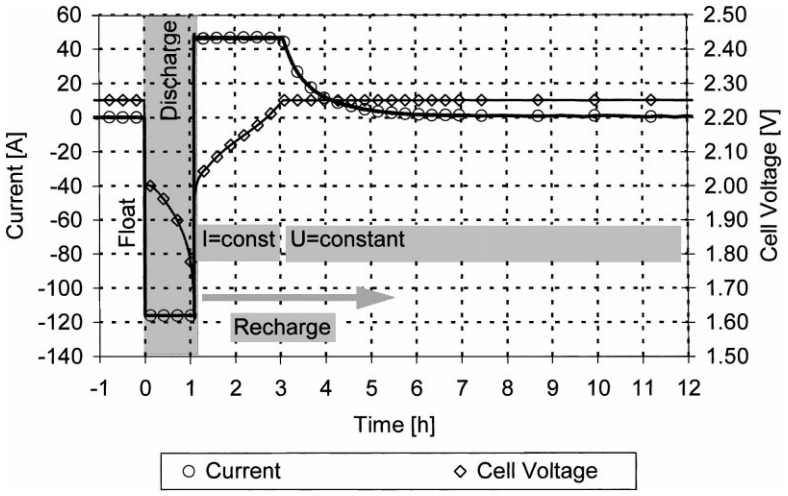

Fig. 2. Voltage and current transients during a constant current discharge with 116 A followed by a constant current, constant voltage charge with 46.5 A and 2.25 Vpc.

rise effect also called 'thermal runaway' which can cause monobloc temperatures of up to 100°C with associated partial melting of the battery container.

Such a runaway condition could be triggered if, during a high rate charge, a significant temperature rise causes the charge current not to drop significantly once the maximum charge voltage limit is reached. The elevated residual charging current can then generate enough heat to overwhelm the heat rejection capability of the monobloc and thus result in either a very high permanent operating temperature ($T > 45$°C) or in a thermal runaway condition with ultimate destruction of the battery.

The evolution of the temperature of each cell of the monobloc was followed by measuring the temperature of the monobloc case with a thermocouple located at the point of maximum heat generation as identified by prior thermal imaging.

The temperature evolution shown in Fig. 3 is that of cell 2 located in the center of the 6 V monobloc. Four section of interest can be discerned.

Section A shows the temperature of the monobloc in above described cubicle during float charge at 2.25 Vpc and ∼100 mA float current. The ambient air temperature was 23°C.

Section B shows the nearly linear temperature rise of approximately 4°C above ambient caused by the 116 A discharge to 1.60 Vpc during which about 50 W of internal heat are generated.

Section C shows the thermally most active region where the largest temperature rise takes place as the result of the inflow of the charging current. The temperature maximum occurs when a recharge status of 87–92% is reached.

With the U = constant charge, resulting in a peak current of 341 A, the maximum heat generation occurs approximately after 1 h since charging started and at a recharge level of 88%.

The key thermal data are summarized in Fig. 4 and Table 1.

Section D shows the decay of the monobloc temperature once the maximum was attained. The decay rate is, with

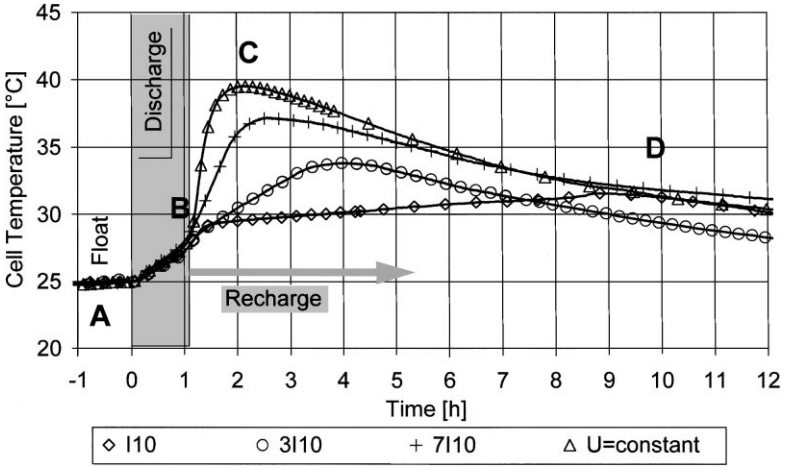

Fig. 3. Evolution of the temperature of the monobloc as function of the charging current magnitude.

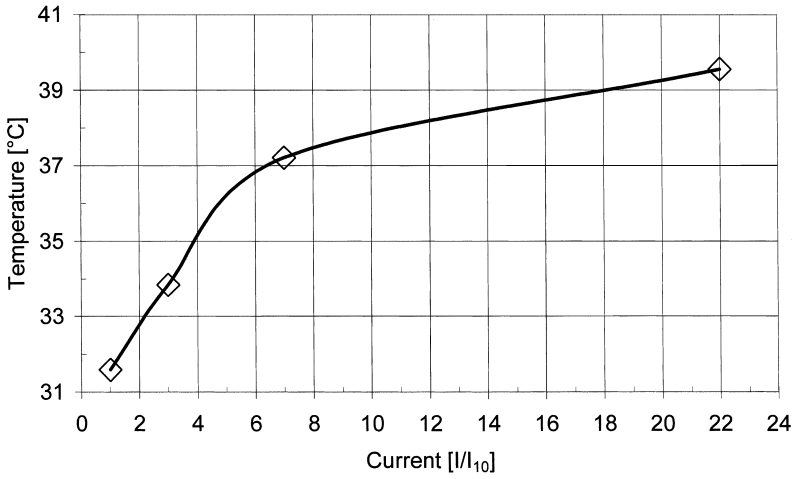

Fig. 4. Maximum monobloc temperature as function of the charging current magnitude.

approximately 0.5°C per hour in the critical time period, quite similar in all the four experiments. Also in the high rate U = constant charge mode the temperature decay was quite pronounced and did not appear to be a harbinger of a future thermal runaway.

3.1.2. Temperature distribution

The evolution of the distribution of the temperature within the monobloc can be determined by thermal video imaging. This method helps in the development of proper cooling strategies and the optimization of internal components.

An image of the temperature distribution was recorded every 1–5 min and stored as digital data file. The PicEd software was used to edit and display the thermal information either as absolute or as differential temperature distribution image.

Fig. 5 shows the image of the localized temperature increases during discharges. This differential image gives optimum sensitivity and was obtained by subtracting, from the temperature distribution image recorded at the end of the 116 A discharge, the temperature distribution image just prior the start of the discharge.

The internal geometry of the three cells with the location of the plate stack and the gas room is clearly outlined.

As visible from this image the maximum temperature rise of 4°C is localized in the upper 1/3 of the plate group and relates to the sites where, due to increasing IR drops further down the plate, the discharge reaction occurs with preference. This differential image reveals also that some plates of the plate group, looked at edgewise, exhibit a slightly higher temperature of +0.5°C than immediately neighboring ones.

Of the top lead consisting of the terminals, plate group straps and through-the-partition weld connectors only the latter one shows a significant localized temperature rise of approximately 4°C.

Fig. 6 shows distribution of the maximum temperature increase resulting for the discharge and the constant current–constant voltage charge with $3I_{10}$ or 46.5 A current and during the U = constant charge and 341 A peak current.

In these two images different temperature inhomogeneities are observed with the localized peak temperatures of +9°C and +15°C, respectively now found deeper down the plate group and slightly more pronounced in the center cell. This differentiation is the result of heat transfer through the top-lead away from the plate group and from the plate group via the monobloc walls to the ambient air.

3.2. Recharge characteristics

A fast recharge of a lead acid battery of the VRLA in UPS service is desirable so to quickly regain the capability to provide power during a possible renewed power outage.

A recharge under float charge conditions of 2.25 Vpc is governed by the apparent internal resistance of the monobloc and how the resulting polarization increases with time.

Table 1
Key thermal data

Charge current (A)	Maximum temperature T_{max} attained (°C)	Temperature rise T_{max} (°C per hour)	Elapsed time of charge at T_{max} (h)	Ampere hours recharged at T_{max} (%)
I_{10} (15.5)	32	0.4	7.7	90
$3I_{10}$ (46.5)	34	2.1	3.0	92
$7I_{10}$ (108.5)	37	6.7	1.5	87
$22I_{10}$ (341)	40	12.6	1.0	89

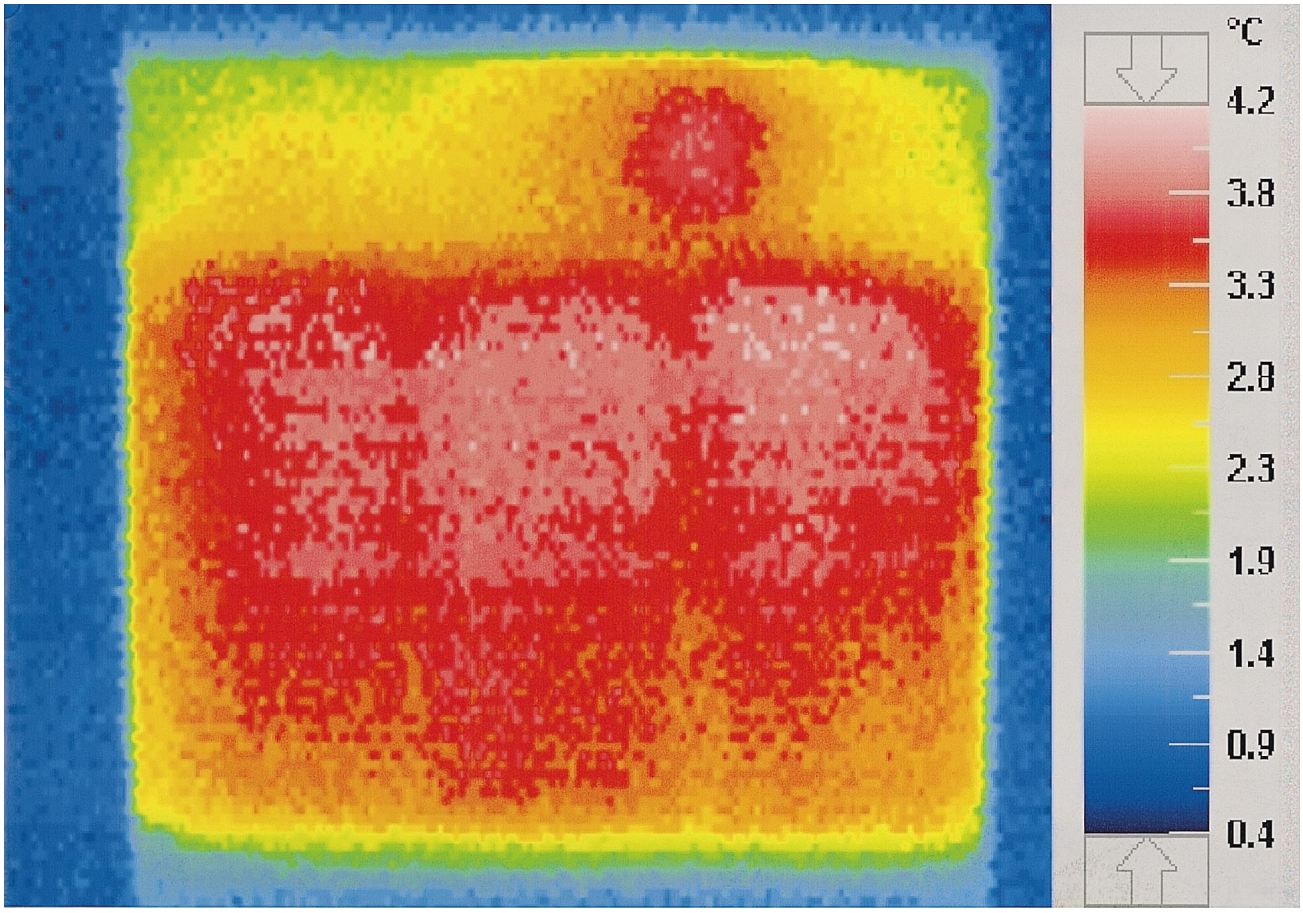

Fig. 5. Thermal image showing the temperature increases due to the 116 A of the constant current discharge to 1.60 Vpc.

The lower this internal resistance is and the slower polarization increases the longer the charge current can replenish the discharged Ampere hours under predictable I = constant conditions.The resulting data for the charging characteristics are displayed in Table 2.

3.2.1. Time to reach a status of full charge

The Ampere hours reintroduced in these high rate recharge experiments were determined by numerical integration of the charging current and are shown in Fig. 7 and Table 2. In the graph the charging time to reintroduce 50, 80

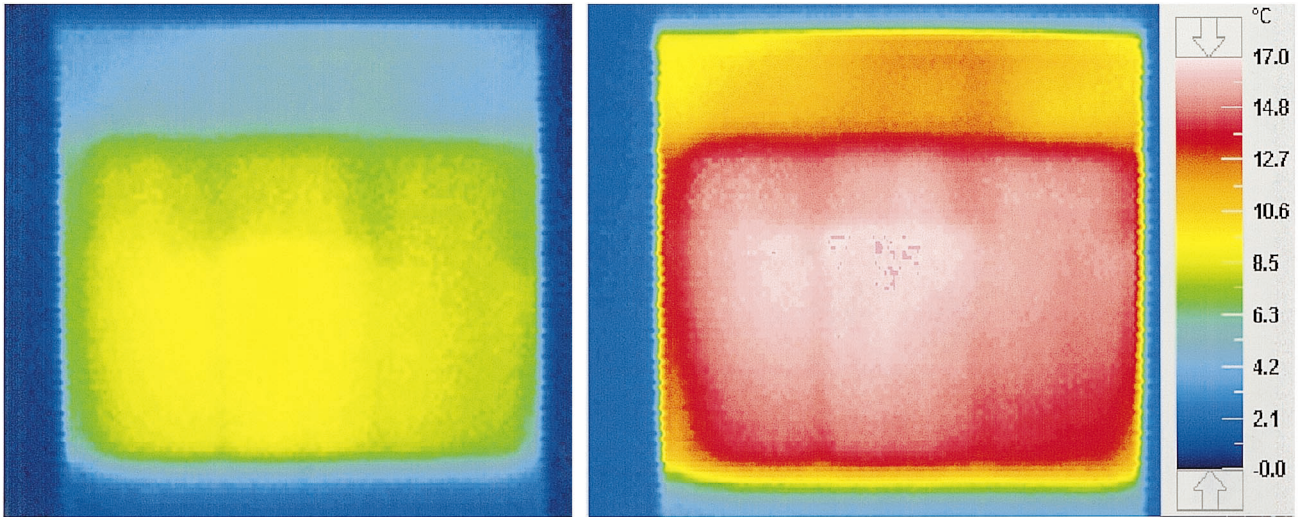

Fig. 6. Localized temperature increase image during the $3I_{10}$ or 46.5 A current charge (left) and during the U = constant 341 A peak current charge (right).

Table 2
Charging characteristics data as a function of the charging current

Charge current (A)	Elapsed time of charge at a charge quotient (h)			Elapsed time of charge to reach 2.25 Vpc (h)	Charge quotient at 2.25 Vpc (%)
	50%	80%	100%		
I_{10} (15.5)	4.2	6.7	11.3	7.3	87
$3I_{10}$ (46.5)	1.3	2.2	6.0	2.0	74
$7I_{10}$ (108.5)	0.6	1.1	4.5	0.6	56
$22I_{10}$ (341)	0.2	0.6	3.1	0	0

and 100% of the previously discharged Ampere hours (116 A h) is plotted versus maximum charging current.

The resulting hyperbola shaped function of time versus current shows clearly the time to be gained by increasing the initial charging current from I_{10} to $3I_{10}$ and further to $7I_{10}$. A further increase of the charging rate by charging under $U =$ constant conditions, associated with a peak current of 341 A, does not significantly improve the speed with which a status of near full charge is achieved.

3.2.2. Time to reach the maximum charging voltage limit

During the recharge, with a maximum voltage equivalent to the float voltage of 2.25 Vpc, the time elapsed before this value is reached corresponds to the constant current phase and correlates with a certain degree of recharge.

This level of recharge is shown in the Fig. 8 were the time to reach the float voltage and the recharge status at this moment, is plotted as function of the initial charging current. Both values of time and recharge status are zero in the case of $U =$ constant charge and rise to 7.3 h and 87% of recharge with $I = I_{10}$. In above discussion the recharge status of 100% is defined as the instant of time when $Ah_{in}/Ah_{out} = 1.0$.

Under high rate discharge/charge conditions this corresponds also the instant of time at which the full autonomy time for power back-up is once more available from the battery. Under particular circumstances, see also [5], full back-up time may be available before 100% of the discharged Ampere hours have been recharged back into the battery.

3.3. Gas pressure and emission during high rate charging

Lead acid batteries of the VRLA type emit gas during all operating conditions. This gas emission has multiple causes and relates to the inefficiencies of the charge reaction mainly at the positive plate, to the hydrogen evolution on the negative plate due to the self discharge reaction and impurities in the electrolyte and to the balance of the corrosion reaction of the lead components of the positive plate.

This gas emission has to be managed for safety purposes so to prevent that an explosive mixture consisting of more than 4% hydrogen in air develops in the vicinity of the battery.

As high rate charges can cause inefficiencies in charging current acceptance a quantification of the gas emission in function of the charging rate was desirable.

3.3.1. Gas pressure within the cell

The monoblocs are equipped with one-way valves for each cell with an opening pressure of 8–10 kPa and a closing pressure of 4–6 kPa.

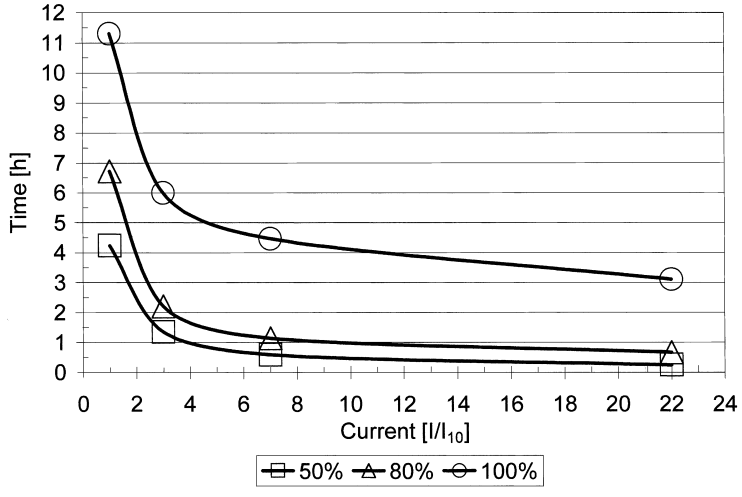

Fig. 7. Recharge time to 50, 80 and 100% of discharged Ampere hour reintroduced.

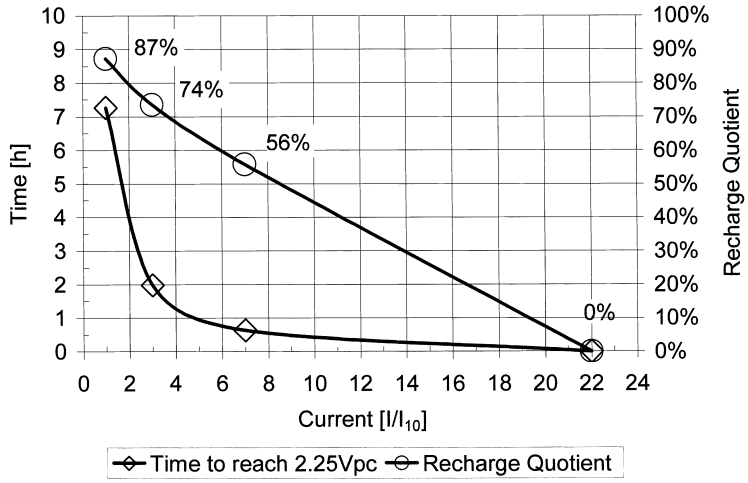

Fig. 8. Time to reach 2.2.5 Vpc and the recharge quotient vs. the charging current.

During the discharge with 116 A to 1.60 Vpc a pressure rise was detectable right from the beginning of each discharge with gas emission occurring once the respective valve opening pressure was reached. This pressure rise is caused by thermal expansion of the gas within the cell, the displacement of gas form the pores by low density lead sulfate discharge reaction product and possibly by the desorption of oxygen from the lead dioxide active material.

The pressure versus time trace during a discharge followed by a recharge with $3I_{10}$ is shown in Fig. 9 and is characterized by five distinctive sections A though E.

Section A corresponds to the steady state pressure condition within the cell during float charge.

Section B corresponds to the pressure rise during the discharge resulting in valve opening at 9 kPa overpressure.

Section C corresponds to the most salient feature of the pressure versus time behavior and shows a pressure decay which magnitude and duration is dependent on the values of the charging current. During a I_{10} charge sequence the pressure decay resulted in a negative pressure, i.e. a partial vacuum in the cell. From this pressure drop and partial vacuum condition it can be inferred that the residual oxygen content in the head gas of the cells is quickly gettered by the negative active material before renewed gas emission occurs in the subsequent phases of the charge. The negative pressure condition requires that the VRLA valve design should be capable to prevent any ingress of atmospheric gases in the cells under such partial vacuum conditions.

Section D corresponds to the pressure rise caused by the onset of gas evolution when the battery reaches a status of charge of approximately 85–90%. This pressure rise results also in some gas venting from the cell.

Section E corresponds a gradual decay of the pressure as further venting from the cell and gettering oxygen by the negative active material causes the cell pressure to drop to a minimal overpressure. This condition of minimal overpressure is followed by a renewed gas pressure rise up to 6–8 kPa under stabilized float charge conditions.

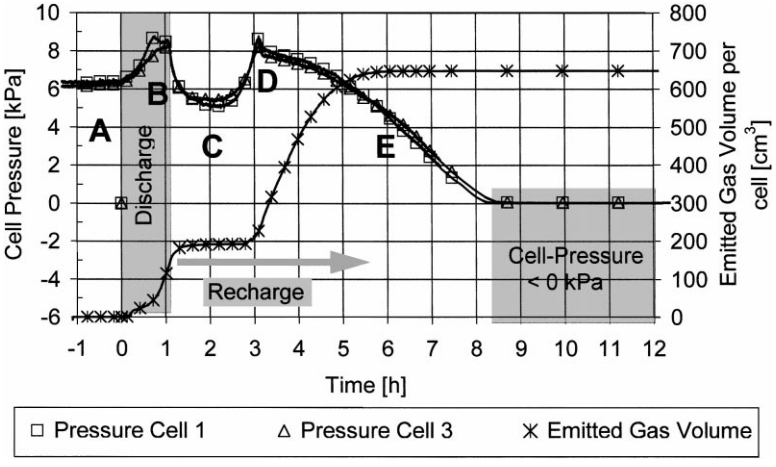

Fig. 9. Evolution of the pressure in the cell and gas emission during discharge and $3I_{10}$ recharge.

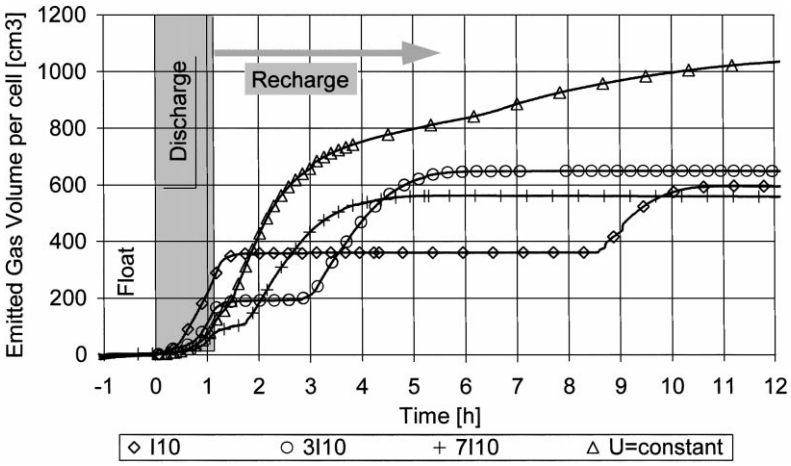

Fig. 10. Timing and quantity of gas emitted as function of charging current magnitude.

Table 3
The emitted gas volumes per cell

Charge current (A)	Gas emitted during the 1 h discharge with 116 A to 1.60 Vpc (ml)	Gas emitted during the recharge to 100% with 2.25 Vpc maximum (ml)
I_{10} (15.5)	350	275
$3I_{10}$ (46.5)	191	466
$7I_{10}$ (108.5)	115	446
$22I_{10}$ (341)	176	976

3.3.2. Gas emitted from the cells

Gas emission occurs from the cells when the internal pressure reaches the opening pressure of the valve. This is happening at the end of the 1 h discharge and when the cells reaches, during charge, the float charge voltage.

The amount of gas emitted is quite small and, in the case of the discharge event, dependent on the length of the previous float charge period.

The gas volume emitted during the discharge varies between 115 and 350 ml depending on the time of float charge since the last discharge event (Table 3). In a typical UPS installation, with this monobloc type and with nominal 480 V, this would amount to potentially 84 l of hydrogen per discharge event to be managed via the battery room ventilation.

The timing and quantity of gas emission at different recharge rates is shown in Fig. 10.

During charge not unexpectedly the highest gas emission is observed under $U =$ constant charging conditions with approximately 1 l of gas emitted. This gas emission equates to a potential water loss, from the electrolyte, of 0.5 g per cell and $U =$ constant recharge event.

3.3.3. Composition of gas emitted from the cells

Gas emission occurs from the cells when the internal pressure reaches the opening pressure of the valve and the composition of the emitted gas can reveal its origin.

The chemical analysis of the gas emitted during the discharge phase contained less than 2% oxygen and is thus assumed to be formed essentially by hydrogen of the cell head volume and gas dislodged from the absorber and negative plate pore volume.

The gas emitted during the charge phase in contrast contained up to 33% of oxygen originating thus from the stoichiometric decomposition of water which yields two volumes of hydrogen and one volume of oxygen.

4. Conclusion

Fast recharging of lead acid batteries of the VRLA type and with absorbed electrolyte (AGM) is feasible without unduly high thermal loads and gas emission.

The experimental results indicate that an initial charging current in the $3I_{10}$ to $7I_{10}$ range allows to recharge a fully discharged monobloc in 4–6 h with its temperature not exceeding 40°C as compared to a recharge with the current limited to I_{10} which rises the temperature to only 32°C but requires up to 12 h to reach a similar state of charge.

The thermal video imaging reveals that during discharge at the 1 h rate to 1.60 Vpc heat generation is concentrated in the upper 1/3 of the plate group and in the through-the-partition weld connector. During charge the highest local temperatures is found in the center of the plate group.

The gas emission occurring during discharge is constituted mainly by hydrogen whereas the gas emitted in the charging phase is hydrogen with 33% of oxygen.

Acknowledgements

The assistance of M. Zeller, H. Bigler and A. Baerfuss of the Innovation and Test Laboratory of Oerlikon Stationary

Batteries Ltd. in Aesch, Switzerland in the execution of the experiments is greatly appreciated.

References

[1] M. Fernandez, F. Trinidad, J. Power Sources 67 (1997) 125–133.
[2] E. Feissner, J. Power Sources 78 (1999) 99–114.
[3] W. Bogner, et al., in: T. Keily, B.W. Baxter (Eds.), Proceedings of the 16th International Power Sources Symposium, Bournemouth (UK) 1988 in Power Sources, Vol. 12, 1989, pp. 703–720.
[4] H. Giess, J. Power Sources 67 (1997) 49–59.
[5] H. Giess, in: Proceedings of the Intelec 2000, 22nd International Telecommunications Energy Conference (Phoenix, Arizona, USA), September 2000, pp. 749–754.